2008

Application of impedance spectroscopy to the study of dithiocarbamate species on Au surfaces: Effects of aqueous Cu^{2+} and Mg^{2+} ions

Tom Riha

Application of Impedance Spectroscopy to the Study of Dithiocarbamate Species on Au

Surfaces: Effects of Aqueous Cu^{2+} and Mg^{2+} Ions

By

Tom Riha

Thesis

Submitted to the Department of Chemistry

Eastern Michigan University

In partial fulfillment of the requirements

For the degree of

MASTER OF SCIENCE

in

Chemistry

Thesis Committee:

Donald Snyder, PhD, Chair

Timothy Friebe, PhD, Committee Member

Larry Kolopaijlo, PhD, Committee Member

July 15th, 2008

Ypsilanti, Michigan

Thesis Approval Form

Application of Impedance Spectroscopy Measurements to Study Dithiocarbamate Anchored

Molecules on Au Surfaces: Effects of Aqueous Cu^{2+} and Mg^{2+} Ions

By

Tom Riha

_____   _____

Donald Snyder, PhD   Date
Thesis Chair

_____   _____

Timothy Friebe, PhD   Date
Committee Member

_____   _____

Larry Kolopaijlo, PhD   Date
Committee Member

_____   _____

Ross Nord, PhD   Date
Department Head

_____   _____

Deborah de Laski-Smith, PhD   Date
Interim Dean of the Graduate School

ABSTRACT

Self-assembled monolayers (SAM) of dithiocarbamate ligands were formed on the Au surface of an interdigitated electrode (IDE) array by reaction of amines with CS_2 in H_2O/CH_3OH solutions. Impedance spectroscopy was used to probe for the presence of each SAM as they were individually applied to the surface of the IDE by examining differences in collected impedance data after each step of the chemical application sequence. The impedance behavior of the SAM's were then studied in the presence of aqueous Cu^{2+} and Mg^{2+} ions. A treated IDE array would, in theory, be able to preferentially detect lower concentrations of Cu^{2+}(aq) by complexing with that specific ion, thus concentrating it within the capacitance field. Cupric ion chelating groups anchored to the gold surface by the dithiocarbamate group included morpholine or 5-amino-1,10-phenanthroline. A sensitive determination of the amount of Cu^{2+} leaching from anti-fouling marine hull coatings into water would be a useful example of practical applications of impedance-based sensors for heavy metal ions. Results of this work indicate that the SAM-treated IDE arrays differed in their impedance behavior relative to untreated IDE arrays. The SAM-treated IDE arrays detected 1.00 μM Cu^{2+} concentrations with confidence, while untreated IDE arrays only detected as low as 50.0 μM Cu^{2+} with confidence.

TABLE OF CONTENTS

LIST OF TABLES

LIST OF FIGURES

CHAPTER 1 – INTRODUCTION

Resistance Behavior of AC Circuits

Impedance is known as the measure of the total opposition to flow of a sinusoidal electric current when using AC circuitry. To better understand what impedance actually is, one can use Ohms law to explain how it's measured. Ohm's law applies directly to simple resistors (and conductors) in both DC and AC circuits. However, in more complex AC circuits, the form of the current-voltage relationship defined by Ohms law must be changed from I=V/R to I = V/Z. Note that V is voltage, I is the resulting current, and R is resistance. The quantity Z for the modified formula is denoted as impedance, which is measured in ohms, and for a pure resistor $Z = R$. Impedance is commonly represented as $Z = R + iX,$ where R is the ohmic resistance and X is the reactance.

Circuit elements such as inductors and capacitors have a frequency dependent opposition to current flow and increase or decrease current opposition as AC frequency changes. The opposition to current flow caused by inductance or capacitance is known as *reactance*. The term *reactance* refers to the imaginary part of the impedance measurement (iX) due to it being a function of the frequency. Generally speaking, a capacitor would have an impedance measurement that would decrease with increasing frequency supplied to the circuit. An inductor would have an impedance value that increases with increasing frequency. Also, a pure resistor would have the same impedance measurement at any frequency applied to the circuit.

When capacitors or inductors are involved in an AC circuit, the current and voltage do not peak at the same time. The period difference between the peaks, expressed in degrees, is known as the phase difference. The contributions of capacitors and inductors differ in

phase from resistive components by 90 degrees. For inductive circuits, this results in a positive phase because current lags behind the voltage while for a capacitive circuit, the current leads the voltage for a negative phase. A resistor does not cause a phase shift. Since the C/V behavior of capacitors and inductors are 180° out-of-phase, the impedance in a given circuit using both elements will have a phase-angle dependence.[1]

Impedance spectroscopy (IS) can provide accurate evaluation of material characteristics by measuring impedance values for a range of circuit elements whose capacitance or inductance characteristics depend in some way on their chemical environment. Impedance vs. frequency data for different electrode configurations is typically collected by connecting the electrode to an impedance analyzer and then graphically presenting the data as either a Bode or Nyquist plot. The Bode graph plots absolute values of impedance (Z) or phase angle (degrees) vs. the frequency range used while Nyquist plots depict the imaginary number Z" (reactance) vs. the real number value Z'. Examples can be viewed in Figs 1 & 2.
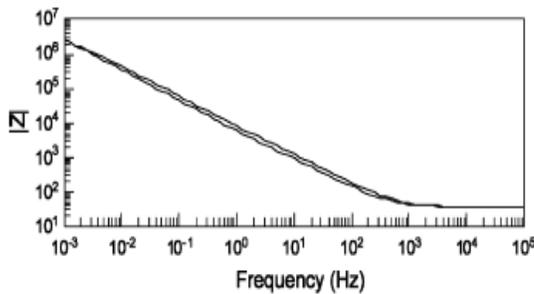
Figure 1: Typical Bode plot (Z vs. Hz).   **Figure 2**: Typical Nyquist plot (Z" vs. Z').
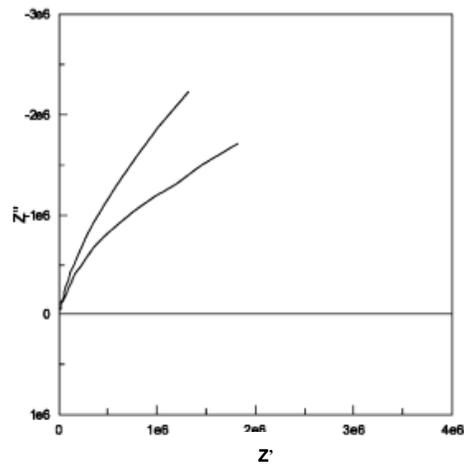
2

The majority of work in this area is based on using interdigitated electrode (IDE) arrays as the AC circuit element responsible for varying impedance. Recent studies have shown that impedance measurements can be related to charge carriers in bulk or interfacial regions, proton/electron conductivity, dielectric constants, charge mobility, equilibrium concentration of charged species, interfacial capacitance, and diffusion coefficients.[2]

Some applications of IDE-based impedance spectroscopy include biosensor development for targeted biomolecules, the study of the conduction of polymer films with varying thickness, corrosion degradation, analysis of proton exchange membranes, and self-assembled monolayers.

Interdigitated Electrode (IDE) Arrays for Impedance Spectroscopy

The general design of an IDE device can be visualized as 2 metal combs lying flat and pushed together so that the teeth mesh without actually touching (Fig 3). The metal leads then function as a surface parallel plate capacitor.[3] The electrode consists of two contact points (cathode and anode), which allow wire connections from fixtures to be made to its leads and directed to an impedance analyzer. Two leads from the contact points on the electrode travel to the array, which is generally the area of interest. The array itself resembles two fine tooth combs pushed together when the effects of a capacitor are desired and the array is the site for measuring the capacitance effects of a sample. Variation in the size of the array will lead to variations in impedance measurements. The general development of micro capacitor arrays has been reported.[4] Designs are currently being implemented for many sensor studies, and some examples are briefly described here to illustrate the general concept.
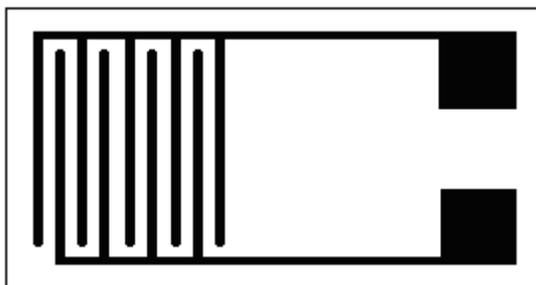
Figure 3: Drawing of an interdigitated electrode. *Left side*: Array. *Right side*: Contact points.

The electrodes array can vary in size depending on the experiment for which the electrode is used. The materials used in the design of the arrays are typically gold or platinum to help prevent unnecessary corrosion.   For proper impedance testing to be conducted, a suitable size for the array must be selected such that the effect of a sample's impedance on the circuit differs significantly from the "baseline" impedance of the array alone. This can be done by testing the electrode/array manually under experimental conditions followed by comparison of data collected when the IDE is not present in its test fixtures. If a suitable difference can be ascertained from the noise reported by the fixtures vs. the IDEs own analysis, the IDE has the potential to be used for the desired experiment.

Sensor Applications Utilizing Impedance Spectroscopy

Impedance spectroscopy has contributed to the development and testing of biosensors over the past few years [5-9] because it can be specific in detecting a given material of interest rather quickly with little sample preparation. This requires a surface that can selectively bind the target molecule from solution with a corresponding change in impedance with varying concentration. One such way to accomplish this is by electrochemically polymerizing films

directly onto the electrode array, which can physically entrap enzymes and other biological materials for selective binding of the target molecule. [5]

Impedance measurements of conducting polymer films can be used to determine a sensor's baseline impedance signature for comparison to the impedance behavior when the IDE is exposed to an analyte solution. [6] Specific immune binding reactions that take place on a surface of a p-Si chip can produce impedance results significantly different from the uncoated IDE.[7] It can also be used to detect DNA hybridization using coatings of polypyrrole on the array as a way to immobilize the DNA to study complementary and non-complementary DNA targets.[8-9]

Impedance spectroscopy can be used to measure the mechanism of degradation for polymers deposited on the surface of an electrode. Double layer capacitance, membrane pore resistance, charge resistance, and doping onto polymers using bulky cations and/or anions and deactivation by overoxidative degradation of Pt can be evaluated.[10] Inorganic salts deposited on platinum electrodes have been found to be good candidates for developing electrochemical sensors for inorganic environments because of their greater resistance to overall degradation as compared to sensors using organics.[11]

Impedance spectroscopy has been used to examine the corrosion of complex 3D titanium foams used for biomedical purposes.[12] It has also been used to study the corrosive degradation of metal barriers by determining changes in the porosity and degradation of applied coatings, specifically polarization and double-layer capacitance, which were used to analyze the delamination of top coatings and the onset of corrosion.[13]

A unique technique for simulating taste has been developed based on impedance spectroscopy where nanostructured films of conductive polymers over an IDE array function

as an ''electronic tongue.''[14] This sensor detected trace organics at levels less than that detected by a human tongue, using gold interdigitated electrodes coated with polypyrrole and stearic acid. Wine has also been studied utilizing the "tongue."[15]

AC impedance spectroscopy has been used to measure the proton conductivity of many different proton exchange membranes (PEM) including Nafion, where it was determined that a combination of H_2O/HSO_3^- ratio and $[H^+]$ gave useful parameters for detecting trends in proton conductivity. [16] The dielectric and electrical behaviors of Nafion have also been examined using impedance spectroscopy as a function of time to determine the water retention of Nafion and other composites at high temperatures.[17] Charge transfer resistance for carbon nanotube based electrodes used for the membrane assembly of proton exchange membranes has also been measured by utilizing impedance spectroscopy.[18]

Self-Assembled Monolayers (SAMs)

Experimental design of specific sensors can require a monolayer treated surface to be employed when used in aqueous environments. The monolayers provide the ability of an IDE to interact selectively with a substance of interest in the aqueous environment. Although molecular monolayers may be deposited on solid surfaces electrochemically, as with conductive polymers, a simpler method relies on spontaneous self-assembly using organic molecules with a particularly strong affinity for the surface. SAMs can be formed by submerging a solid material (like Au) into a solution of another material (such as CS_2) which adsorbs onto the surface. Since the process is quite easy to implement, it makes the process attractive for quick fabrication of monolayer treated surfaces.[19, 21] Outcomes using SAMs have been very favorable due to their ability to have a high level of specificity for various chemical structures, molecular size relationships, and interfacial phenomena.[19-20]

Specifically, they offer great insight onto interactions at interfaces due to their great ability to produce order and unique orientation for adsorbed molecules in applications for chemical and bio chemical sensor development. [20-21]

Such organic derivitized metal surfaces are commonly used in surface science, nanomaterials and chemotherapeutic research.[22] Self-assembled monolayers of thiols attached to gold surfaces are an example of a common use of SAMs. It has been reported that CS_2 groups possess high chemisorption properties due to sulfur-to-sulfur bond distances, which are ideal for adsorption onto gold.[23] This is made even more advantageous due to the ability of CS_2 to react with a secondary amine forming dithiocarbamates, which then bind onto the Au spontaneously. The secondary amine/CS_2 reaction with subsequent Au adsorption has been demonstrated for a variety of amines.[22] These could be used to aid the analysis of certain samples that require chelators in order to concentrate the analyte of interest near the electrode surface. A logical extension of this concept uses the dithiocarbamate to anchor a Cu^{2+}- specific chelator to the gold IDE surface.

Impedance Behavior of IDE in the Presence of Mobile Ions

A capacitor stores energy in an electric field between its conducting plates, with the magnitude of stored charges directly related to the dielectric constant of the insulating medium between the plates. This electric field can be altered by the interaction of metal ions entering the field, changing the dielectric constant and thus altering capacitance, and hence, the impedance as well. Presumably, at very low concentrations, there would be too few ions to have a significant effect, but if a suitable chelating agent is part of a self-assembled monolayer attached to the metal surface, it should concentrate the metal ion inside the capacitance field and cause a change in the measured impedance. The magnitude and

7

frequency behavior of this expected impedance change is difficult to predict since the mechanism is subject to many variables. When the IDE is charged, each electrode will have its fluid double layer with opposite ion orientation (see Fig.4).
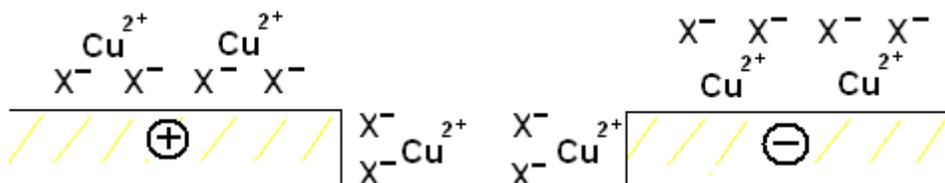
Figure 4: Charged IDE illustrating electrodes fluid double layer with opposite ion orientation.

Reversing the charges during the AC cycle would require extensive ion reorientation in the double layers, introducing time and ion mobility dependence factors. Concentrating the metal ions close to the surface by chelating of the SAM will undoubtedly alter these effects significantly. This thesis project explores the effect on impedance of an IDE with surface-anchored chelating groups in the presence of aqueous metal ions as a potential method for detection and quantitation of such ions.

CHAPTER 2 – EXPERIMENTAL PROCEDURES

All experimental data were collected using an Agilent HP 4192A LF impedance analyzer with an HP 16047A test fixture. All data were acquired by a 6-minute frequency sweep from 5 Hz to 13 MHz at a constant 0.02 V applied to the IDE chip arrays. Laboratory temperature was between 19°C to 21°C during all testing. Small fluctuations in temperature caused no change in reproducibility of the data collected. Electrical connections to the IDE chips relied primarily on spring loaded clips pressed securely onto surface contact pads at the chip edge, with the chip oriented to allow immersion of the array surface in test solutions as shown in Figs. 5 & 6.
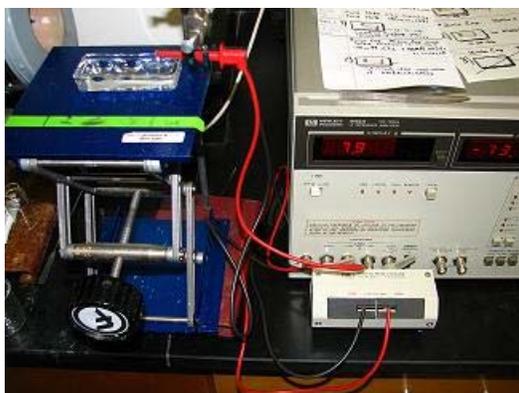
Figure 5: J-hook attached & submerged IDE array.

Figure 6: Impedance analyzer setup.

The interdigitated electrode arrays were manufactured by photolithography with a spacing of 10 microns between 10 micron panel leads, with a thickness of approximately 1000 Å. Note that three different types of capacitor arrays were tested during the experiments, all of which had varying surface area for their arrays. Below are descriptions of the arrays used:

PTI Array: Commercial SiO_2 passivated silicon wafer coated with gold with an array surface area size of 6.30 mm^2. These arrays were extensively tested but eventually discarded due to the poor electrical characteristics related to the manufacturing process, as well as their excessive brittleness.

Abtech 1050.5 Array: Made of gold on glass manufactured by photolithography. A given array surface area is 9.58 mm^2. A smaller Abtech array (designated 1025) was also tested. Their overall design was durable and the array was well made, consistent, and produced impedance data with a favorable difference in values from that of an empty test clip, but due to their very high cost not enough of them could be obtained for the entire research project.

U of M Array: Made of gold on glass with an array surface area of 19.6 mm^2. These arrays were manufactured at the University of Michigan photolithography lab and were used for the bulk of the experimental work of this research. Their array was the largest, which made them the most sensitive to alterations of their electric field. The array area was composed of leads 10 microns thick, which alternated with 10 micron spaces. Approximately 500 total leads are present in the array.

<u>HP Impedance Analyzer Data Collection</u>

Customized labview software titled "SWEEPER" was used to control the HP analyzer and collect data. This software was originally developed at the IRC Institute for Biomedical Materials Queen Mary-University of London and was used with their permission. Data included impedance values and signal phase angle as a function of frequency with an AC voltage of 0.02 V from 5 Hz to13 MHz. Raw data from SWEEPER were collected and placed in an EXCEL file and converted into graphical plots for either Z (impedance) vs. Hz, phase angle vs. Hz, or a combination of the two when needed.

<u>Copper and Magnesium Samples</u>

Cu^{2+} & Mg^{2+} solutions were prepared from $CuSO_4*5H_2O$ and anhydrous $MgSO_4$. Both were dissolved in deionized H_2O to produce 50.00 ml samples in appropriate volumetric glassware. The concentrations used for both ions were 25mM, 5mM, 1mM, 0.5mM, 0.1mM, 0.05mM, 0.01mM, 0.005mM, and 0.001mM.

<u>SAM Samples</u>

For treatment of the U of M arrays, pure HPLC grade CS_2 was applied first for assurance that the array would be fully coated with a base monolayer, followed by a 100mM sample of morpholine or 5-amino-1,10-phenanthroline in CH_3OH. Their structures can be viewed in Figs. 7 & 8, respectively.
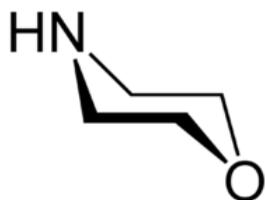
Figure 7: Morpholine (C_4H_9NO).   **Figure 8:** 5-Amino-1,10-Phenanthroline ($C_{12}H_9N_3$).
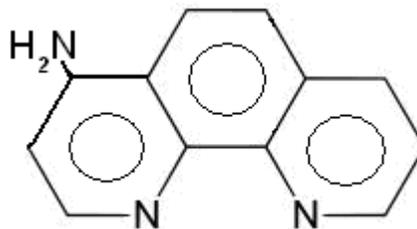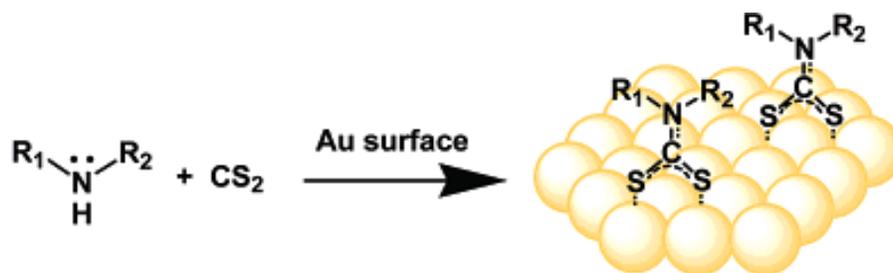
Figure 9: Illustration of SAM formation.

The IDE array areas were submerged into the chemical solutions described above to form the SAMs. Carbon disulfide was used first to create a layer favorable for a second compound to be added that would bind to the carbon in CS_2 along with a second group, which had lone pairs of electrons to interact with a metal ion in solution (R1 & R2 in Fig. 9). Treatment was done by submerging the array of the IDE for 20 minutes in pure CS_2 followed by a minimum of a 10 minute dry time. After CS_2 treatment, the array was submerged in either 100mM morpholine or phenanthroline for building the desired SAM for analysis of metal ions. Examples of various other secondary amine/CS_2 reactions with subsequent Au adsorption have been conducted.[22]

CHAPTER 3 – RESULTS & DISCUSSION

1.   Empty Test Clip

Initial work began by determining the background impedance and phase angle values produced by the standard sweep conditions on the wiring set-up without the IDE chip in the circuit. The test fixture was an alligator type clip with four metal contact points located at intervals across the square jaw front such that clamping the edge of the IDE chip in the jaw tip pressed the connectors onto the chip contact pads. Standard J-hook clips were then placed on the appropriate leads to connect the chip array to the impedance analyzer.

A number of standard runs were made on the empty test clip, and all sets of raw data obtained were identical in impedance and phase angle vs. Hz sweep collected, as shown in the log-log plot of Fig. 10.
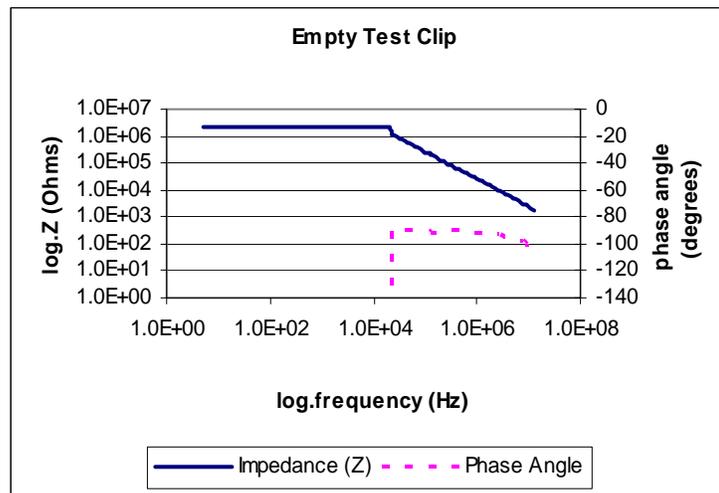
Figure 10: Typical data collection of Z & phase angle vs. Hz for empty test clips.

2.   Selection of IDE Array
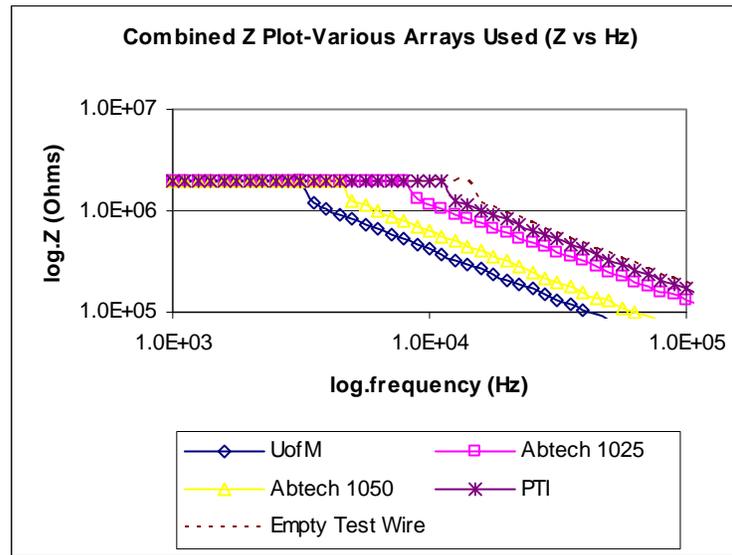
Figure 11: Combined plot of impedance vs. Hz for blank arrays and empty test wire

When the new IDE arrays were obtained, they were examined microscopically to ensure that their dimensions were correct (10 micron spacing). Analysis began by comparing the Z data obtained by a standard frequency sweep for each array. Fig. 11 shows that the new UM array with its larger array surface area produced the lowest Z data at a given Hz point and also produced the greatest difference from the empty test wires, being about 600 ohms less. The greater magnitude in ohms difference was expected to aid in the ability to detect smaller amounts of metal ions in solution when in contact with the array's electric field since this IDE was more conductive (lower Z) than previous ones. With its larger array area and lower cost, the UM IDE chip was chosen for all subsequent experiments.

3.   Alternate IDE Chip Connection Method

Since the impedance behavior of the test system is a function of the capacitance of

both the IDE and the connecting wires, an alternate method of connecting the chip to the HP

4182A unit was tested in an effort to minimize the extraneous capacitance of the alligator

clip. For this test, standard J-hook connectors were clipped directly to the contact pads on

the IDE chip edge and a standard sweep run for comparison. The wires were found to

provide slightly overall lower Z data than that of the test clip (Fig. 12) although the

difference in parasitic capacitance was very small. The more secure connections of the J-

hook wire assembly were deemed valuable to experimental reproducibility and to achieving

minimum parasitic capacitance, hence removing the need for the alligator clip.
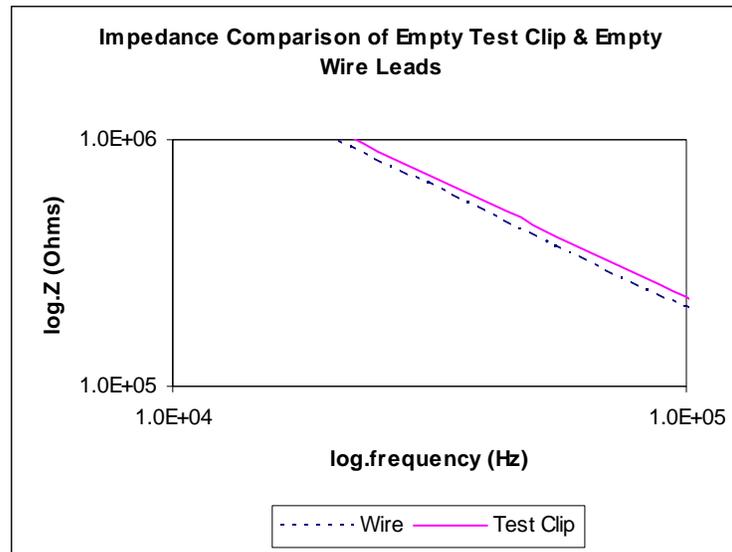
Figure 12: Impedance analysis of empty test clip vs. wire leads.

4. Initial Tests on Z Behavior of IDE Array in Aqueous Environment

a. Deionized (DI) H$_2$O Sample Application Methods

Two methods were tested for exposing the IDE array to test solutions. The first was surface application via microsyringe of a 2 μl droplet over the horizontal array area surface (Fig. 13).
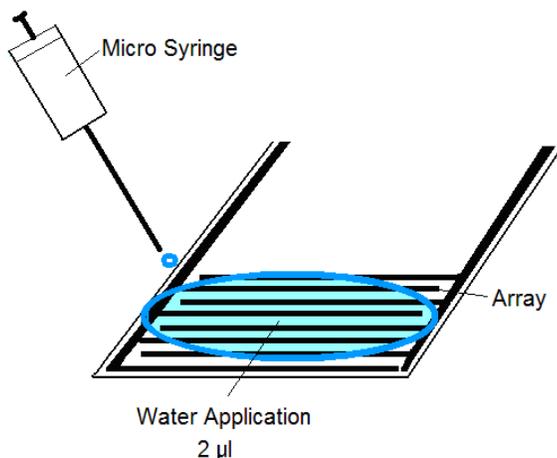
Figure 13: Application of 2 μl H$_2$O sample onto array surface using a micro syringe.

The second was vertical immersion of the chip end into a small volume of the solution. The surface application technique was found to have reproducibility problems, which appeared to be related to evaporation of the 2 ul droplet during the 6-minute run time.

Figs. 14 & 15 contrast impedance plots for application vs. immersion of the IDE array with DI H$_2$O. These were also generally similar in profile but had noticeable differences in both Z values and phase angle over the frequency range.
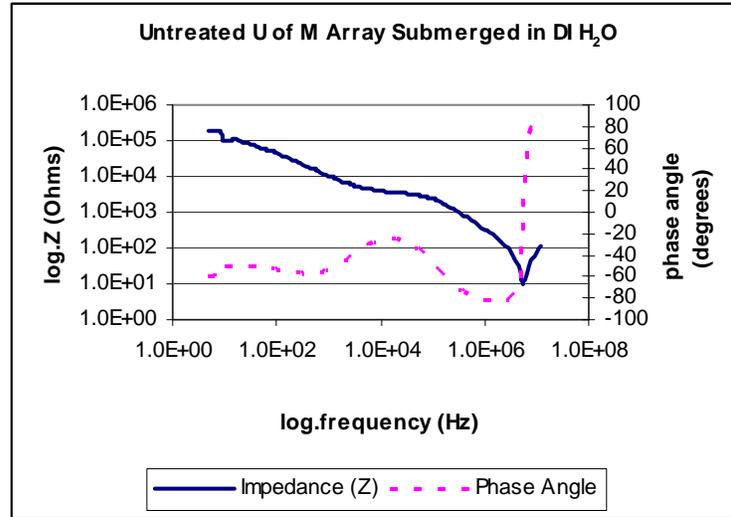
Figure 14: Analysis of array submerged in DI H_2O.
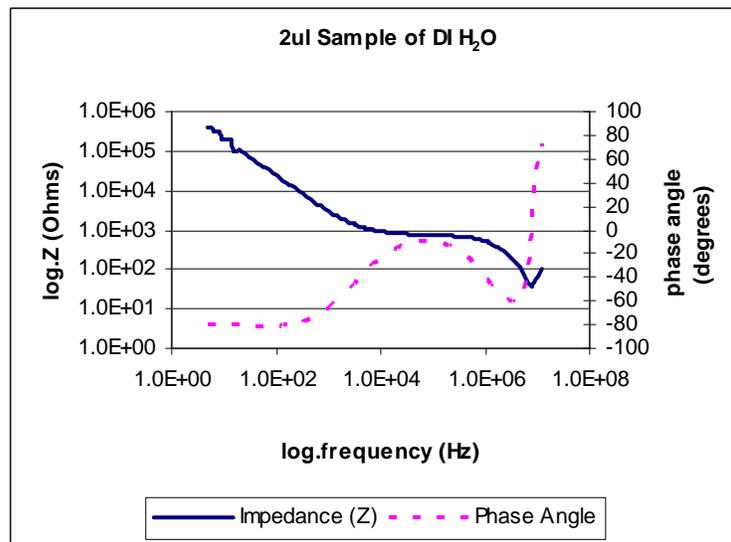
Figure 15: Analysis of array applied with 2ul sample of DI H_2O.

In comparison to the runs in which a 2μl sample was placed on the array (Fig. 15), submerged arrays (Fig. 14) produced a Z data plot with a deeper valley between 6-7 MHz when analyzed and a smaller max for phase angle between 3-5 MHz. The data collected by submersion were reproducible, and repeated runs gave identical impedance plots each time.

17

It is apparent that reversing the potential during the alternating current cycle on the IDE must create a constant changing of the H_2O molecular orientation at the metal surface. A comparison of Figs.11 & 14 clearly demonstrates that the effect of a polar liquid like water on the impedance response of the IDE is pronounced. As with any capacitor, the polar liquid between the array leads (the plate equivalents) increases charge storage capability by increasing the dielectric constant. Within the electric fields adjacent to the metal leads, the dipole moment of the water molecules orients in the appropriate direction to stabilize the alternating charges, as shown in Fig.16.
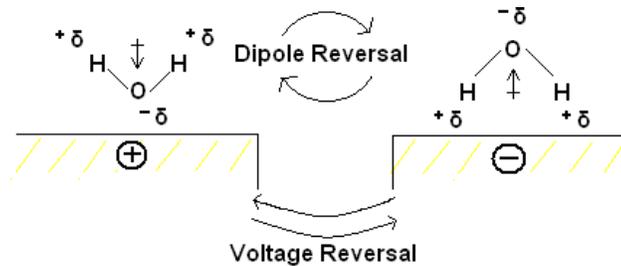
Figure 16: Charged IDE illustrating AC interaction/attraction of H_2O using dipole moments. Reversing the lead potentials during the AC current cycle requires that the water dipoles reorient to the opposite alignment. The decrease in impedance over the sweep range indicates that this induced rotation of the water molecules becomes more efficient as the AC frequency increases, reaching a maximum (minimum Z) between 5-6 MHz. While it is tempting to equate this to a matching of the quantized rotational frequency of gas-phase H_2O molecules, the fact that the process is occurring in a condensed phase renders such a view overly simplistic.

b. **Cu^{2+} and Mg^{2+} mM Samples Using Untreated UM IDE's**

A comparison of 25mM Cu^{2+} and Mg^{2+} show impedance plots between

1.0E+2 and 1.0E+7 Hz, which are significantly different from deionized H$_2$O (Fig

17).
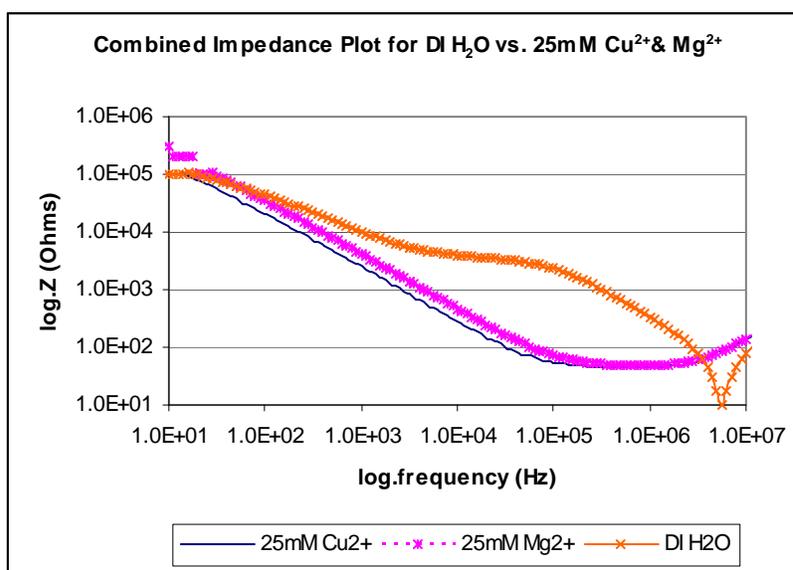
Figure 17: Comparison of 0.025M Cu^{2+} & Mg^{2+} samples vs. DI H$_2$O.

The H$_2$O plot shows higher Z values relative to the dilute aqueous Cu^{2+} & Mg^{2+}

solutions from the initial sweep frequency up to 6 MHz. This is consistent with the

theory that charged species should decrease measured impedance values over a broad

frequency range by increasing the dielectric constant of the medium.

Since the Z vs. frequency plots for pure H$_2$O and metal ion solutions have

different curvature, the numerical relationship between Z and ion concentrations will

depend on the exact frequency chosen for comparison. In the absence of other

specific criteria, the choice of frequency must be, to some extent, arbitrary. The

impedance signal for the aqueous metal ion solutions is a function of both the pure

H$_2$O baseline and the added effect of the dissolved ions. In order to look for small

19

changes in Z with [M+], it was decided to use the frequency (6-7 MHz) at which the background impedance due to pure H_2O was at its minimum (highest conductivity).

c.   **Limit of Detection** **for Metal Ions Using Blank Arrays**

Analysis of DI H_2O was conducted using three different IDE arrays to obtain 9 data plots for Z vs. Hz by using them on alternating days along with removal and reconnection of the arrays before analysis. Examination of the impedance plots while analyzing the Cu^{2+} samples had shown that between 5 & 6 MHz the Z data formed a local minimum. The bottom of the Z data valley can be clearly seen at 5623413 Hz. As concentration of Cu^{2+} decreased, the Z data valleys for untreated or treated arrays decreased to approach a DI H_2O Z data plot (Fig. 18).

From the nine samples of H_2O analyzed, the average Z at the given point was 9.82 ohms. The limit of detection (LOD) was calculated using the program Excel to determine the standard deviation from the data collected and gave a value of $\pm$1.30. The LOD obtained (1.30 ohms) was then used as a guide to determine how dilute a metal ion concentration could be when approaching the DI H_2O Z data at 5623413 Hz and still show a distinguishable reading. For example, if Z data for DI H_2O at 5623413 Hz was 8.6 ohms, the data point for the Cu^{2+}solution would have to exceed 9.9 ohms to be considered detectable. Anything below 9.9 ohms would be indistinguishable from DI H_2O. The Z values at the minimum for the nine plots from the nine sets of data can be seen in Table 1.

	Array 1a	1b	1c	Array 2a	2b	2c	Array 3a	3b	3c
Impedance (Ohms)	9.9	9.4	9.1	9.71	9.44	10.1	10.25	10.3	10.21

Table 1: Z data from DI H_2O samples used for determining LOD for treated arrays.

Additional impedance runs with immersion in Cu^{2+} (aq) solutions of varying concentration showed a distinct effect on the Z value at that frequency (5623413 Hz) that could be correlated with concentration, as seen in Figs. 18 & 19.

d. Correlation of [Cu^{2+}] & [Mg^{2+}] with Z

Array Design	Array Area	Substrate	Sample	Metal	Concentration (mM) of Metal Analyzed
U of M	19.6 mm	None	DI H_2O	Cu^{2+}	1, 0.5, 0.1, 0.05,0.01,0.001 & DI H_2O

Table 2: Experimental conditions for an untreated array with Cu^{2+} samples.
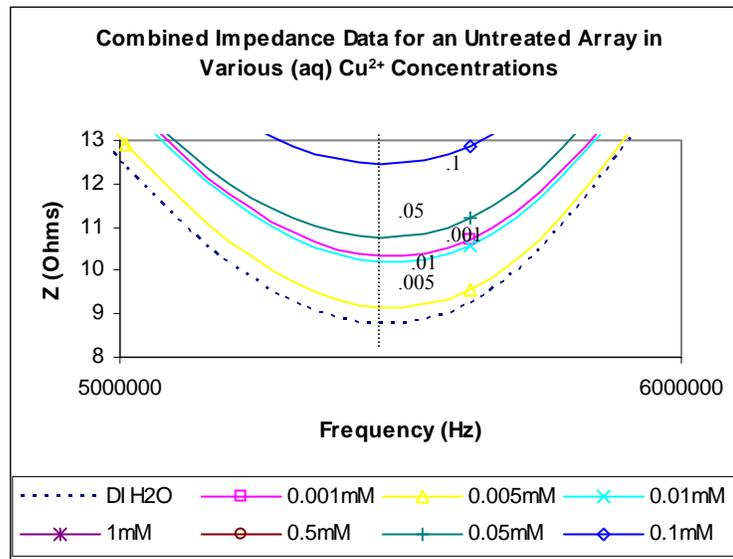
Figure 18: Comparison of Z curves as a function of [Cu^{2+}].

Fig. 18 shows Z decreasing as concentration decreases the for 0.1mM and 0.05mM Cu^{2+} samples; however, samples 0.001mM, 0.01mM, and 0.005mM are not in a decreasing order as they approached the DI H_2O plot. It was expected that as concentration decreased the plots would approach that of DI H_2O, but repeated trials with untreated arrays often gave plots that failed to correlate with decreasing concentration of Cu^{2+}. The 0.001mM data plots were often found at a higher Z than

0.01mM samples, and in some cases entire plots had been shifted to the right to fall

between 6-7 MHz instead of the normal location of 5-6 MHz.

Array Design	Array Area	Substrate	Sample	Metal	Concentration (mM) of Metal Analyzed
U of M	19.6 mm	None	DI H_2O	Mg^{2+}	0.1, 0.05,0.01,0.001 & DI H_2O

Table 3: Experimental conditions for an untreated array with Mg^{2+} samples
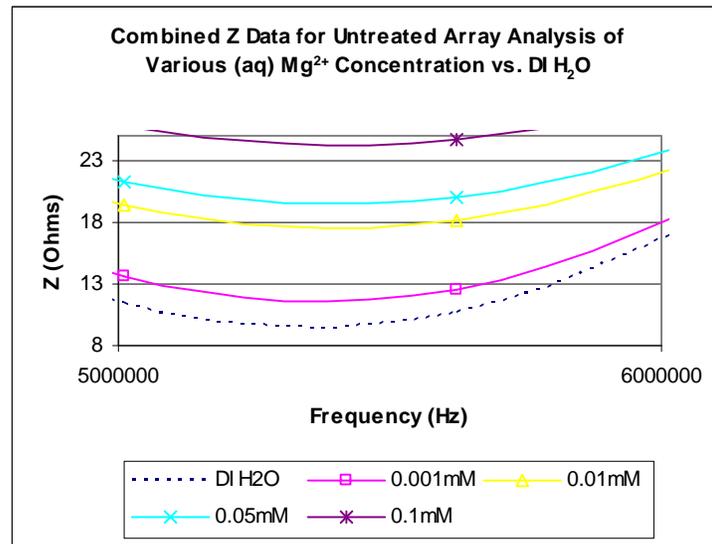
Figure 19: Impedance analysis of Mg^{2+} samples with an untreated array.
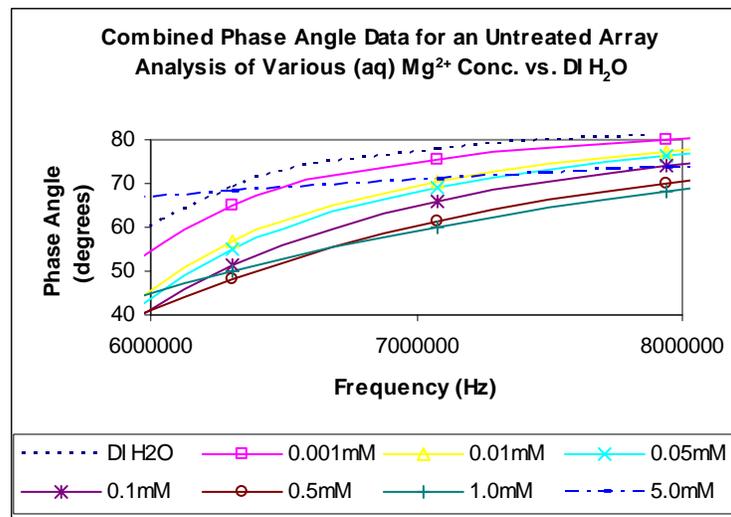
Figure 20: Phase angle analysis for Mg^{2+} samples with an untreated array.

The phase angle vs. Hz plot (Fig. 20) was produced to show that the Z &

phase angle data plots gave similar correlations; the difference being that the phase

angle vs. Hz curves for each $[Mg^{2+}]$ showed a consistent increase instead of the valley

minimum seen in prior graphs. The phase angles vs. Hz plots were not generated for

every experiment because they were repetitive to what impedance vs. Hz plots

revealed by way of plots approaching the DI H_2O data collected for comparison to the

LOD.

5.   **Z Behavior of SAM Treated IDE Arrays in Aqueous Environment**

       a. SAM formation using CS_2, Morpholine, & Phenanthroline

       The chemical treatment for developing the self-assembled monolayer was

used in order to create a surface that would bind to the gold that made up the array

and also bind selectively to the metal ions in solution which, in turn, would allow

smaller concentrations of Cu^{2+} to influence the IDE electric field and alter the

impedance response. The initial set of experiments using the treatment was done to

determine if the chosen chemicals would indeed bind to the array and would change

the Z & phase vs. Hz behavior in some consistent manner relative to the untreated

blank array.

       The first step of the treatment in building the SAM used CS_2 alone. Thiols

and other oganosulfur species are well known to adsorb onto gold surfaces very

strongly just from solution contact. Pure CS_2 was used to insure full coverage of the

Au leads. The starting array was first washed with acetone and allowed to air dry,

then attached to the test clip. The test clip was held in place by a clamp that was used

to hold the array so that it could be held upright and completely submerged in a liquid

sample. A small glass plate with small wells was used to house the liquid samples for treatment. The CS$_2$ sample was used to fill the glass well, and the array was submerged until it touched to bottom of the well plate. The array end of the chip was submerged in the sample for 2 minutes and then removed and allowed to air dry for 5 minutes.

The second step used morpholine, so that its amine nitrogen would attach to the monolayer of CS$_2$ while the oxygen on the opposite side of its ring could then be used to interact with metal ions in solution due to the lone pair electrons on the O (Fig. 21). The Z behavior of the array was determined after each step in the process to determine any changes due to the adsorbed species. The thin film made by the SAM that had been adsorbed onto the surface of the IDE could be anchored and detected repeatedly with success. The following material describes this in detail (Fig. 21).
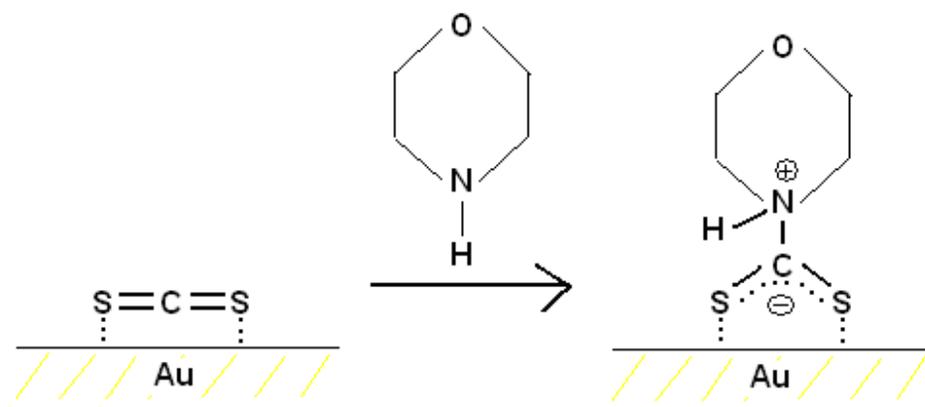
Figure 21: Formation of a SAM using pure CS$_2$ & 100mM morpholine.

The morpholine/CS$_2$ treated array was then submerged in a 5mM Cu^{2+} solution and a standard impedance sweep performed. An overall comparison of plots, treated and untreated, can be seen in Fig. 22.
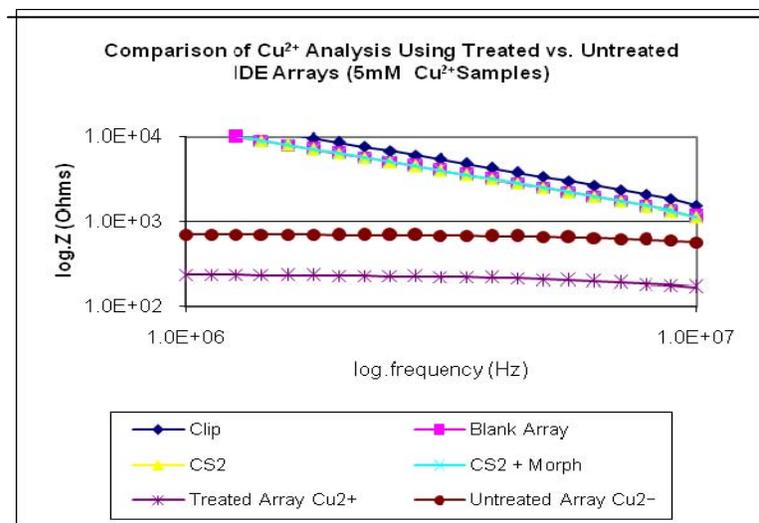
Figure 22: Analysis of building a SAM followed by analysis of a Cu^{2+} sample.

Fig. 22 demonstrates that using the SAM of morpholine generated a significant difference in the impedance plot when exposed to dilute Cu^{2+} (aq) relative to the blank or untreated IDE array. The effect of the CS_2 alone, and after combination with morpholine, was very small. This suggests that a single monolayer of either CS_2 or the dithiocarbamate species has only a minor influence on the array capacitance. However, the Cu^{2+} test using the CS_2 plus morpholine array is very clearly distinguishable from the untreated array under the same conditions, producing indirect evidence for the presence of the dithiocarbamate surface monolayer. Similar stepwise experiments on SAM formation were done for the other amine to look for evidence of the presence of adsorbed dithiocarbamates.

Figs. 23 & 24 compare a blank array vs. an array treated with CS_2 and either morpholine or 5-amino-1,10-phenanthroline. Expanding the Z scheme magnifies the small differences between treated and untreated arrays, but in both cases, the amine-treated final species consistently had a larger effect than the adsorbed CS_2 alone. Note

that the frequency range is not the same for Figs. 23 & 24. The best Hz range chosen

for the graphs in both cases was that which gave the most defined Z difference.
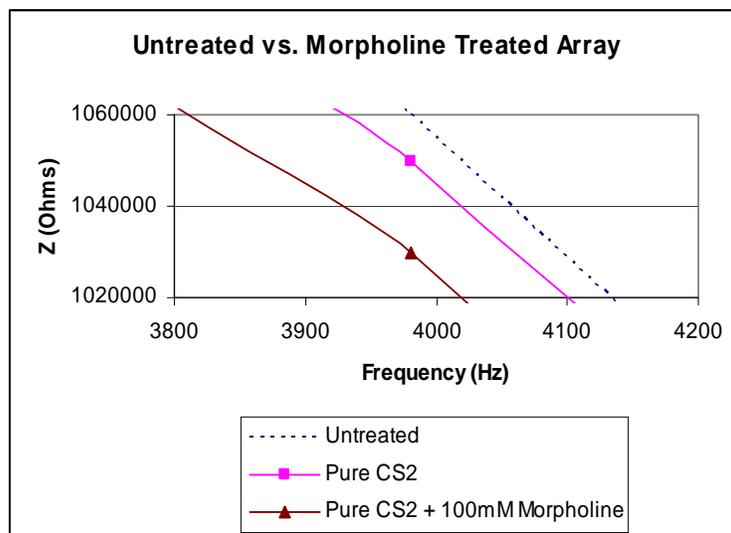
Figure 23: Z analysis morpholine treated vs. non-treated array for evidence of SAM.
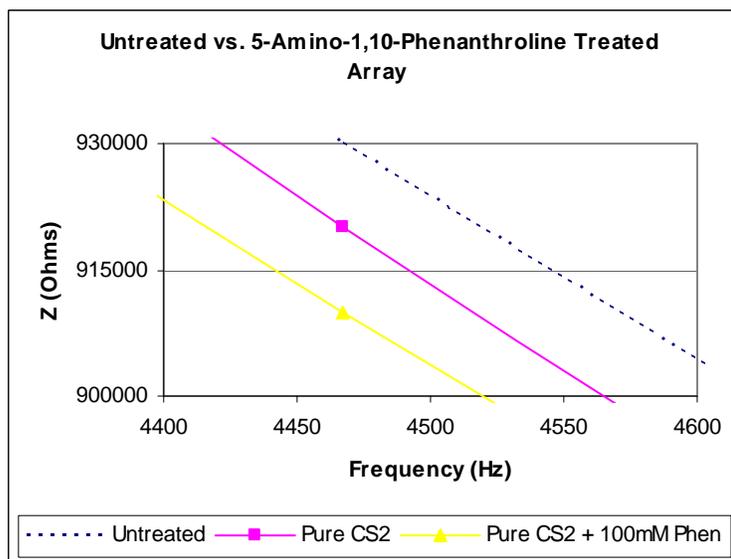
Figure 24: Z analysis phenanthroline treated vs. untreated array for evidence of SAM.

b. **Effect of Cu^{2+} (aq) on SAM of CS$_2$ & 100mM Morpholine**

Array Design	Array Area	Substrate	Metal	Concentration (mM) of Metal Analyzed
U of M	19.6 mm^2	Morpholine	Cu^{2+}	0.1, 0.05, 0.01, 0.001 & DI H$_2$O

Table 4: Experimental conditions for morpholine treated array with Cu^{2+} samples.
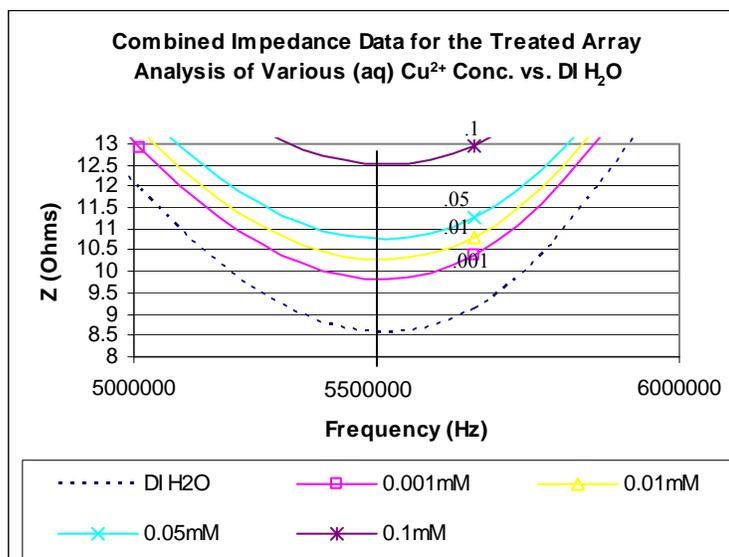
Figure 25: Cu^{2+} samples analyzed with a treated array (CS$_2$ & Morpholine).

With the morpholine/CS$_2$ treated array, the Z values decreased as Cu^{2+} concentration decreased for all samples tested (Fig. 25). The smallest Cu^{2+} sample detected with success and reproducibility was 0.001mM, due to the data point at 5623413 Hz being 1.30 ohms (LOD) greater in value from the H$_2$O Z data obtained while using the same array. While using the untreated arrays, 0.01 and 0.001 mM samples were either out of the order of smaller concentration approaching the H$_2$O plot or the data plots were found to be randomly placed lower or higher in Hz than what was normally detected. The data from Fig. 18 show the disorganization of the data plots.

c.   **Effects of Mg^{2+} (aq) on SAM of CS_2 & 100 Mm Morpholine**

Array Design	Array Area	Substrate	Sample	Metal	Concentration (mM) of Metal Analyzed
U of M	19.6 mm	Morpholine	DI H_2O	Mg^{2+}	0.1, 0.05, 0.01, 0.001 & DI H_2O

Table 5: Experimental conditions for a treated array with Mg^{2+} samples.
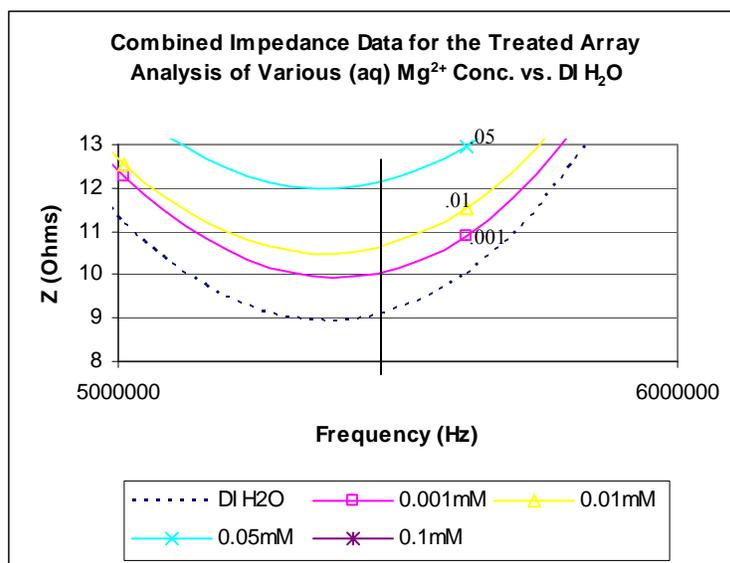
Figure 26: Mg^{2+} impedance analysis with a treated array (CS_2 & Morpholine).

The lowest concentration for Mg^{2+} analyzed was 0.001mM, and its plot (Fig. 26) was found under the limit of detection while using the SAM consisting of CS_2 and morpholine, so detection was considered to be unsuccessful for 0.001mM Mg^{2+}.

d.   **Effect of Cu^{2+} on SAM of CS_2 & 100mM Phenanthroline**

Array Design	Array Area	Substrate	Sample	Metal	Concentration (mM) of Metal Analyzed
U of M	19.6 mm	Phenanthroline	DI H_2O	Cu^{2+}	0.1, 0.05, 0.01, 0.001 & DI H_2O

Table 6: Experimental conditions for phenanthroline treated array with Cu^{2+} samples.

Fig. 27 revealed that treatment allowed the Cu^{+2} sample of 0.001mM to be detected while analysis with an untreated array using the 0.001mM sample was

unsuccessfully analyzed because the data point at 5623413 Hz was not greater than

1.30 ohms from the data obtained for DI H_2O.
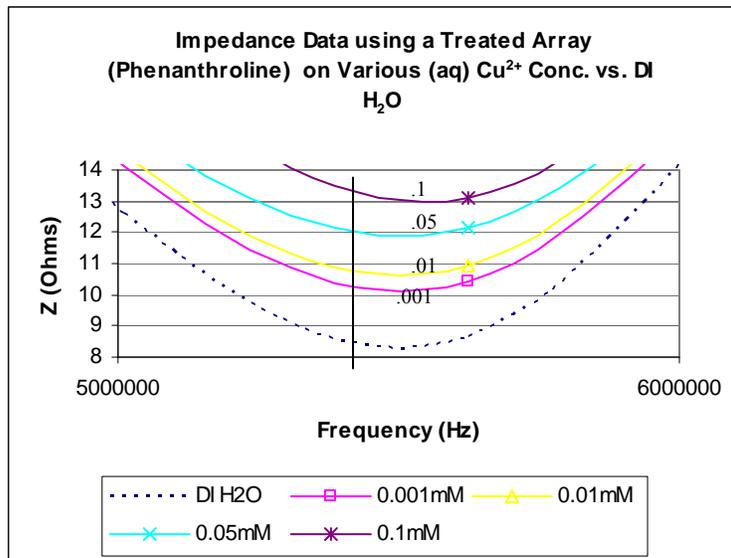
Figure 27: Treated array (Phenanthroline) impedance analysis of Cu^{2+} samples.

Special attention was noted because the phenanthroline-treated array seemed

to have increased the magnitude between 0.001mM sample and H_2O by more than

1ohm than when using morpholine, therefore allowing a greater distance from Cu^{2+}

sample data vs. DI H_2O data favoring the LOD (1.30 ohm difference).

e.   Effect of Mg^{2+} on SAM of CS_2 & 100mM Phenanthroline

For Mg^{2+} samples (Fig. 28), the phenanthroline treatment did not allow the

Mg^{2+} sample of 0.001mM to be detected with confidence due to the data point being

less than 1.30 ohm from the DI H_2O plot.
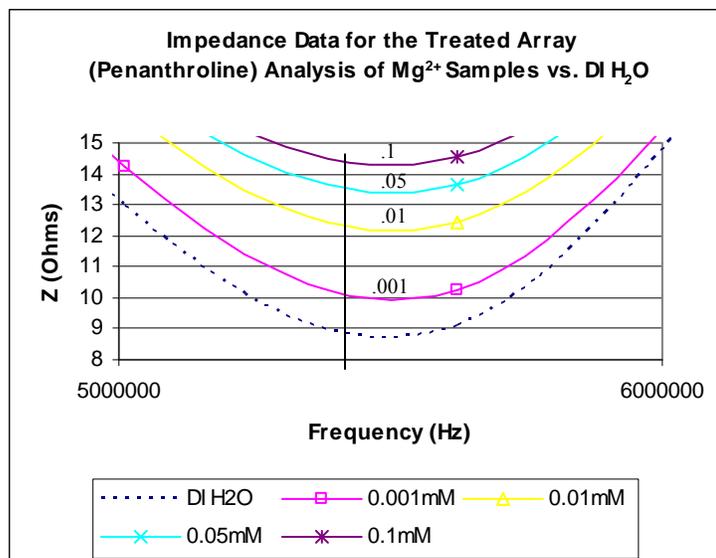
Figure 28: Treated array (Phenanthroline) impedance analysis of Mg^{2+} samples.

The data of 0.001mM Mg^{2+} fell under the LOD at 5623413 Hz. The

phenanthroline did not increase Z data for the sample of 0.001mM and H_2O. Table 7

summarizes the raw impedance data at frequency point 5623413 Hz for Cu^{2+} and

Mg^{2+} samples, which has then been compared to the impedance data of DI H_2O

collected during the same experiment. The difference in ohms between the metal ion

samples and that of DI H_2O revealed which sample and treatment allowed a

successful detection of metal ions by being above (successful) or below

(unsuccessful) the LOD.

	Morpholine (ohms)	Phenanthroline (ohms)		Morpholine (ohms)	Phenanthroline (ohms)
Cu^{2+}	10.48	10.62	Mg^{2+}	10.90	10.26
DI H_2O	9.14	8.82	DI H_2O	10.00	9.12
Difference	1.34	**1.80**	Difference	**0.90**	1.14
LOD (1.30)	Above	Above (Highest)	LOD (1.30)	Below (Lowest)	Below

Table 7: Z comparison of 0.001mM Cu^{2+} & Mg^{2+} vs. DI H_2O at 5623413Hz.

6. Impedance vs. Concentration Comparison

a.   Cu^{2+} Samples

Fig. 29 showing morpholine data and Fig. 30 using phenanthroline plot the impedance values versus the concentration of the samples used by selecting Z values at a fixed Hz point.
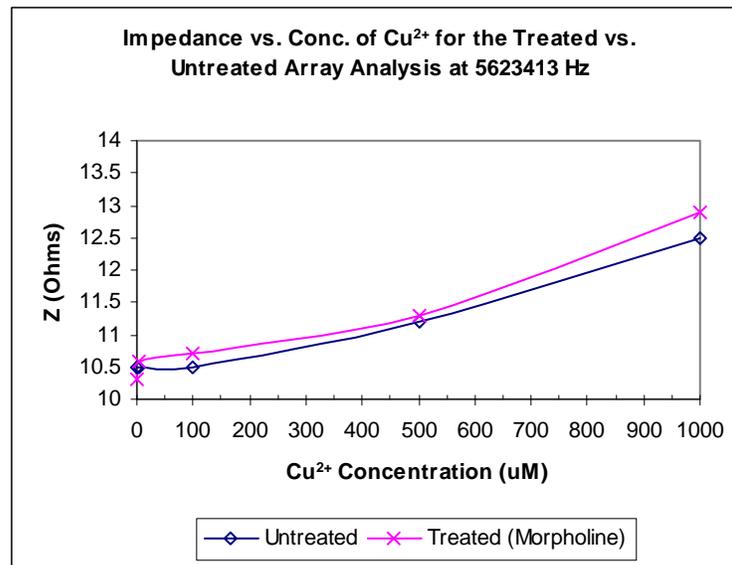
Figure 29: Z vs. conc. analyzing Cu^{2+} with treated (morpholine) & untreated arrays.
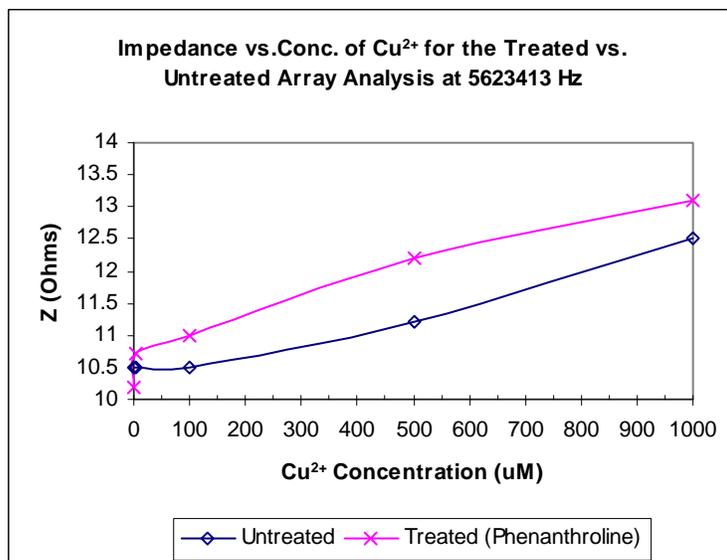
Figure 30: Z vs. conc. analyzing Cu^{2+} with treated (phenanthroline) & untreated arrays.

The frequency used was 5623413 Hz where the greatest change was visually found in the raw Z data. Using phenanthroline to form the SAM used for analysis of Cu^{2+} samples increased the impedance values obtained, hence decreasing overall conductivity of the capacitor. Data from the treatment of morpholine had a minimal impact on increasing Z, so more conductivity was found.

b. **Mg^{2+} Samples**

Data found in Fig. 31 using morpholine and Fig. 32 when using phenanthroline show specific characteristics after plotting the impedance values vs. the concentration of the samples used by selecting Z values at the fixed Hz point of 5623413 Hz.
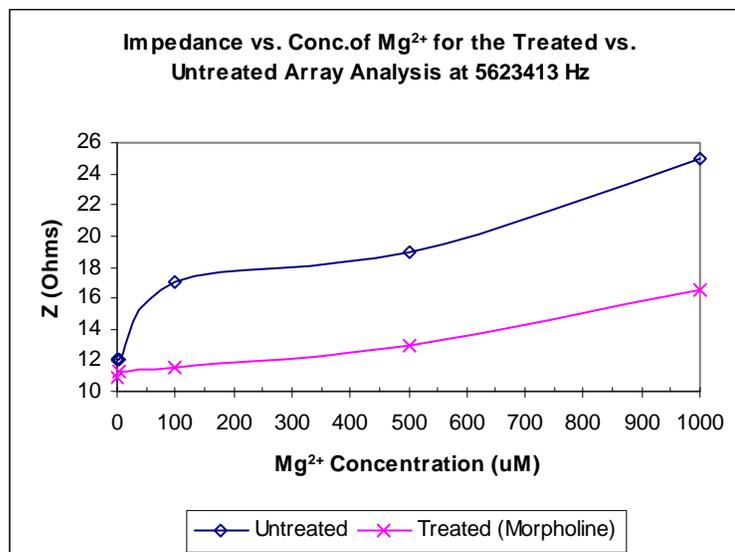
Figure 31: Z vs. conc. analyzing Mg^{2+} with a treated (morpholine) & untreated array
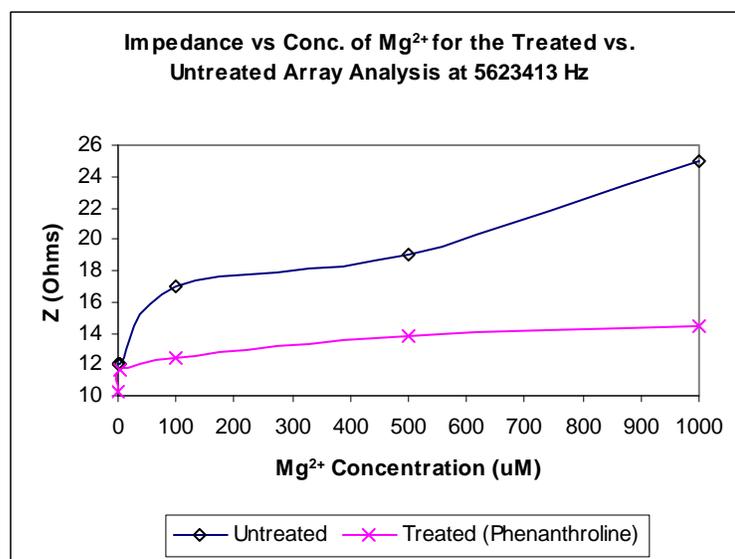
Figure 32: Z vs. conc. analyzing Mg^{2+} with a treated (phenanthroline) & untreated array

When investigating Mg^{2+} samples, it was determined that using morpholine to form the SAM used for analysis decreased the impedance values obtained (Fig. 31), hence increasing reported conductivity of the IDE, making it act more like an insulator. The data from the treatment of 5-amino-1,10-phenanthroline (Fig. 32)

reported a slight increase to the treated Z plot in comparison to the morpholine treated

Z analysis (Fig. 31), which reported lower Z values at the same frequencies.

The SAMs anchored on the IDE interacted with Cu^{2+} to alter the Z data in a

consistent manner related to which SAM was used. Phenanthroline increased the Z of

Cu^{2+} by several ohms vs. using an untreated IDE, while morpholine caused a much

smaller increase. Using either SAM increased the overall Z data with increasing

concentration of Cu^{2+} when compared to an untreated IDE. Mg^{2+} samples had little

interaction to alter the Z when using both types of SAMs since Z data were

indistinguishable between the SAMs used. Various concentrations of Mg^{2+} samples

analyzed using either SAM were found to be consistently lower than using untreated

IDEs.

CHAPTER 4 – SUMMARY & CONCLUSIONS

Changes in the impedance spectra of gold micro-IDE arrays can be correlated with the formation of dithiocarbamate species from the combination of functionalized amines and carbon disulfide. Adsorption of these molecules on to the metal surface through specific interaction of the dithiocarbamate sulfurs with the exposed gold atoms results in significant changes in the impedance and phase angle curves relative to the untreated starting array. The overall change can be followed in a two-step process, which presumably forms a self-assembled monolayer.

The first application of pure CS_2 to the gold IDE array gave a small drop in impedance after drying. Additional application of selected amines (morpholine or 5-amino-1,10- phenanthroline) provided further downward shifts in the plotted impedance vs. frequency curves, as shown in Figs. 22-24. It was clear that the addition of CS_2 lowered the overall Z, and either morpholine or phenanthroline decreased the overall impedance of the array further. These results are consistent with the expected general decrease in Z as the CS_2 binds to the surface as a neutral species. The polarizability of the surface monolayer should increase the dielectric constant of the interfacial region, increasing the charge-storage capacity of the metal and hence lowering the impedance relative to the bare metal.

In the second step, reaction of the amine with the surface-adsorbed CS_2 to form the zwitterionic dithiocarbamate would give an even larger increase in the surface region dielectric constant to further decrease Z. The concentrations of the CS_2 and amine solutions were theoretically sufficient to insure saturation of the gold surface, but a detailed investigation of the actual surface coverage was not undertaken. With impedance data supporting the formation of stable dithiocarbamate monolayers on the gold array surface, the

impedance behavior of the derivatized IDE chips was then studied as a function of aqueous Cu^{2+} and Mg^{2+} concentration.

In order to accurately assess the effect of surface-anchored chelating groups on the impedance behavior of IDE arrays exposed to aqueous solutions of metal ions, the interaction of bare gold leads (without the organic monolayers) with such solutions was studied to determine a baseline for comparison. Standard impedance spectra, plotting both Z and phase angle as a function of frequency, were acquired for multiple dilutions of stock Cu^{2+} and Mg^{2+} solutions. In both systems, the impedance and phase angle curves converged in a reproducible manner toward the curves for pure water, clearly indicating that the effects of the aqueous metal ions were additive with the background effect of the water alone. With the bare gold surface, equivalent concentrations of the two divalent cations showed little significant difference in their impedance plots, indicating that the interaction of the cations with the metal surface in the interfacial boundary layer is primarily nonselective, i.e., more a function of simple charge than the nature of the charged atoms. Repeated tests showed that the lowest concentration of metal ions that could be reliably differentiated from pure water using the blank (underivatized) array was approximately 0.1 mM. Impedance spectra from the same set of sample dilutions were then acquired using the morpholine and phenanthroline-based dithiocarbamate-derivatized IDEs to determine if the presence of suitable chelating groups would increase the detectability limit of the aqueous ions. In order to maintain consistency between the various experimental series, comparison of solution Z values was made at a single, arbitrarily-selected frequency of 5623413 Hz, corresponding to the point at which the impedance of pure water reached its minimum value. This was done to

determine how readily small differences in Z due to varying ion concentrations could be distinguished when the background dielectric effect of water was at its strongest.

The IDE array was used for determining the smallest possible ion concentration that could be reliably analyzed using self-assembled monolayers. A limit of detection was found (1.30 ohms) from using multiple data analysis of deionized H_2O, the same water used to make aqueous metal ion samples, which meant that any impedance data collected for Cu^{2+} or Mg^{2+} samples at the selected frequency of 5623413 Hz had to be 1.30 ohms greater in value than that of the smallest DI H_2O data point at that same Hz, otherwise the sample would be considered deionized H_2O due to data points being so close in proximity (Table 1).

Ion Analysis Using SAM CS_2 & Morpholine

Cu^{2+} samples (0.1, 0.05, 0.01, 0.005 & 0.001) mM were analyzed using the IDE array treated with pure CS_2 & 100mM morpholine. Fig. 25 shows the common trend in how all Cu^{2+} samples produced organized data plots in relation to a sample's concentration when analyzed using the SAM treated array. The untreated arrays produced unorganized data plots that followed no pattern in relation to sample concentration (Fig. 18). For treated arrays in the frequency range of 5–6 MHz, the Z decreased as concentration of the tested samples decreased. The smallest Cu^{2+} sample detected with success was 0.001mM. The data were found to be reproducible, showing where plots had become uniform with smaller concentrations of sample approaching the deionized H_2O plot.

Mg^{2+} samples were analyzed using an untreated array for Z and phase angle data vs. Hz (Figs. 19 & 20). The lowest concentration analyzed for Mg^{2+} was 0.001mM, and its data was found under the limit of detection (1.30 ohms) as compared to that of the DI H_2O data while examining the Z vs. Hz plot. The smallest concentration analyzed for Mg^{2+} was 0.001

mM, and its plot was found <u>under</u> the limit of detection while using the treated array (values found under the LOD were considered undetectable, see Table 7). The smallest concentration determined with certainty was the 0.01mM Mg^{2+} sample while using the treated array with morpholine (Fig 26).

Morpholine reported the lowest Z difference at 5623413 Hz between DI H_2O and 0.001 mM Mg^{2+} with a difference of 0.9 ohms, well below the LOD of 1.30 ohms. When analysis of trace ion concentration in a sample was sought after, a treated array made of morpholine did not allow successful detection of 0.001mM Mg^{2+} samples above the LOD while analysis of Cu^{2+} using a morpholine treated IDE successfully detected the Cu^{2+} by providing data above the LOD at the same frequency and concentration (Table 7).

Ion Analysis Using SAM CS_2 & Phenanthroline

Cu^{2+} samples (Fig. 27) revealed that SAM treatment allowed the Cu^{+2} sample of 0.001mM to be detected while analysis with an untreated array did not allow the 0.001mM sample to be successfully analyzed because it fell under the LOD (1.30 ohms) from DI H_2O data. In particular, it was noted that the phenanthroline increased the distance between the Z data points for the 0.001mM sample and DI H_2O as compared to when using morpholine, allowing for possible greater sensitivity in detecting Cu^{2+} (Table 7).

For Mg^{2+} samples (Fig. 28), the treatment did not successfully detect 0.001mM Mg^{2+} because it fell under the LOD, just as the untreated array analysis of Mg^{2+} 0.001mM was undetectable since it too fell under the LOD. All impedance data used for comparison to deionized H_2O using the LOD can be viewed for Mg^{2+} & Cu^{2+} 0.001mM samples in Table 7.

Ion Concentration vs. Impedance

When comparing impedance data vs. ion concentration, Cu^{2+} samples using phenanthroline in the SAM increased the impedance values obtained, which decreased overall conductivity of the capacitor (Fig. 30). The treatment of morpholine (Fig. 29) impacted the reported Z less than when using phenanthroline. Both morpholine and phenanthroline reported higher impedance data vs. untreated data when comparing Z vs. concentration. When comparing the two SAMs used, Phenanthroline caused the greatest increase in the overall Z when compared to using an untreated IDE to analyze Cu^{2+} samples.

Using morpholine to form the SAM used for analysis of Mg^{2+} samples decreased the impedance values obtained when comparing Mg^{2+} samples vs. the collected untreated Z data, hence increasing conductivity. The data from the treatment of 5-amino-1,10-phenanthroline (Fig. 32) reported only a very slight Z increase in comparison to the morpholine treated Z analysis (Fig. 31), which reported lower Z values at the same frequencies. Both morpholine and phenanthroline reported impedance data below the untreated plots when analyzing Mg^{2+} samples, the direct opposite to what was found when using Cu^{2+} samples, and Z differences between each SAM used was miniscule.

Trends Related to Ion Concentration vs. Impedance

As noted previously (p. 8), it had originally been anticipated that the presence of metal ions such as Cu^{2+} would decrease the impedance (i.e. increase conductivity) of the IDE array by enhancing the ion double-layer at the Au surface, increasing charge storage capacity. This behavior was observed at frequencies from 5 Hz up to ~ 1 MHz. The Z curve minimum between 5-6 MHz for Cu^{2+} solutions of varying concentration, however, demonstrated the opposite effect. Instead of decreasing Cu^{2+} concentration causing Z to rise

until it reached the pure water value, the decreasing Cu^{2+} concentration resulted in <u>lowering</u> of the Z until it matched the pure water value. It seems probable that the effect of dissolved metal ions (with their substantial hydration spheres) in this high frequency range could result from ion-mobility effects in the boundary layer since this would be consistent with a time-dependence of the double-layer reorientation as electrode polarity is alternated. If the electrode charging/discharging rate is at a frequency exceeding ion mobility, double layer charge reorientation would lag behind the sweep frequency and, if sufficiently out-of-phase, tend to hinder electron movement in the Au leads, thus increasing the reactive resistance.

<u>Results of Primary Interest</u>

1. Impedance spectroscopy could be successfully utilized to detect the presence of a monolayer of dithiocarbamate-anchored species on the surface of a gold electrode from CS_2/amines, which were reliably detected from their effect on Z of the IDE arrays.

2. For both the untreated and dithiocarbamate-functionalized IDE arrays, the background impedance of pure water showed the same curves, consisting of a general, non-linear decrease from 5 Hz to a minimum Z at approximately 5.6 MHz, and then a general increase up to the maximum sweep frequency of 13 MHz. The localized minimum is most likely related to an optimum rotational frequency of liquid-phase water molecules allowing for a maximum dipole reorientation rate under the experimental conditions.

3. While impedance plots for aqueous metal ion solutions have consistently lower Z values than pure water for both the untreated and dithiocarbamate-functionalized IDE arrays, the overall curves run roughly parallel until the frequency approaches the 5.6

MHz minimum for pure water. The metal-ion solution Z curves bottom out at approximately 1.0 MHz and then rise slowly until they cross the pure water Z curve at approximately 4 MHz and remain above the pure water curve to the end of the sweep range. The reason for this behavior at higher frequencies is unclear, but speculation centers on limited mobility of the metal ions due to their extensive hydration spheres.

4. In both frequency regimes the effect on Z was primarily non-selective, with the Cu^{2+} and Mg^{2+} at equivalent concentrations showing little difference.

5. SAM and Cu^{2+} interaction was significant with the IDE seen from the increase in Z with increasing concentration of Cu^{2+} while SAM and Mg^{2+} interaction was minimal with the IDE from the lowering of Z with increasing concentration of Mg^{2+}.

6. The success of anchoring SAMs onto UofM IDEs brought about the detection of metal ion samples in smaller concentrations than without the use of SAMs. Mg^{2+} 0.001mM samples could not be detected with confidence since the impedance data for Mg^{2+} fell under the LOD (+1.30 ohms from the Z data point for DI H_2O at 5623413 Hz) while Cu^{2+} 0.001mM impedance data was found to be above the LOD, which represented a successful detection of sample.

7. For Mg^{2+} the smallest concentration successfully analyzed was 0.01mM, and for Cu^{2+} the smallest concentration successfully analyzed was 0.001mM when using treated arrays made from pure CS_2 & 100mM morpholine treatments. When using the treatment of pure CS_2 and phenanthroline, the 0.001mM samples of Cu^{2+} were detectable above the LOD, while the 0.001mM samples of Mg^{2+} still were not. The smallest concentration for Mg^{2+} successfully analyzed was 0.01mM and for Cu^{2+} the

smallest concentration successfully analyzed was 0.001mM using treated arrays made

from pure CS_2 & 100mM phenanthroline (Table 7).

Future experiments are needed to determine if any other SAM formations or capacitor

array designs could be implemented to improve the detection of smaller concentrations of

metal ions present in solution, to find a favorable SAM that could selectively weed through

and detect a specific ion while in the presence of several other heavy metal ions and/or

contaminants, and to determine the cause of the unexpected conductivity trend possibly

related to double layer charge reorientation and ion mobility.

References

1.　Turner, R.P, and Gibilisco, *Principles and Practices of Impedance*, 2nd Edition, Tab Books, Inc., Blue Ridge Summit, PA, 1987.

2.　*Impedance Spectroscopy : Theory, Experiment, and Applications*; Barsoukov, E., MacDonald, J.R., Eds.; John Wiely & Sons, Inc., Hoboken, NJ, 2005; 3.

3.　Sung, J.; Kim, S.; Lee, K. Fabrication of all-solid-state electrochemical microcapacitors. *J. Power Sources* **2004,** 133, 312-319.

4.　Sung, J.; Kim, S.; Lee, K. Fabrication of microcapacitors using conducting polymer electrodes. *J. Power Sources* **2003**, 124, 343-350.

5.　Bartlett, P.N.; Cooper, J.M. A review of immobilization of enzymes in electropolymerized films. *J. Electroanal. Chem.* **1993**, 362, 1-12.

6.　Lyons, E.G.M.; Lyons, H.C.; Fitzgerald, C.; Bannon, T. Poly(pyrrole) based amperometric sensors; Theory and characterization. *Analyst* **1993**, 118, 361-369.

7.　DeSilvia, S.M.; Zhang, Y.; Hesketh J.P.; Maclay, G.J.; Gendel, M.S.;Stetter, R.J. Impedance based sensing of the specific binding reaction between Staphylococcus enterotoxin B and its antybody on a ultra-thin platinum film. *Biosensors & Bioelectrics* **1995**, 10, 675-682.

8.　Hang, T.C.; Guiseppi-Elie, A. Frequency dependant and surface characterization of DNA immobilization and hybridization. *Biosensors & Bioelectrics.* **2004**, 19, 1537-1548.

9.　Tlili, C.; Korri-Youssoufi, H.; Ponsonnet, L.; Martelet, C.; Renault, N. Electrochemical impedance probing of DNA hybridization oligonucleotide-funtionalized polypyrrole. *Talanta* **2005**, 68, 131-137.

10.　Refaey, S.A.M.; Schwitzgebel, G.; Schneider. O; Electrochemical impedance studies on oxidative degredation, deactivation and reactivation of conducting polymers. *Synth. Metals*. **1999**, 98, 183-192.

11.　Fernandez-Sanchez, C.; McNeil, J.C.; Rawson, K. Electrochemical impedance spectroscopy studies of polymer degradation:Application to biosensor development. *Trends in Anal. Chem.* **2005**, 24, 37-48.

12.　Menini, R.; Dion, M.; So, V.K.S.; Gauthier, M.; Lefebvre, L.P. Surface and corrosion electrochemical characterization of titanium foams for implant applications. *J. of the Electrochem. Soc.* **2006**, 153, 1, B13-B21.

13. Suay, J. J.; Rodriguez, M. T.; Razzaq, K.A.; Caprio J. J.; Saura, J. J. The evaluation of anticorrosive automotive epoxy coatings by means of electrochemical impedance spectroscopy. *Progress in Org. Coating.* **2003**, 46, 121-129.

14. Riul, A.; Malmegrim, R. R.; Fonscea, F. J.; Mattoso L.H.C. An artificial taste sensor based on conducting polymers. *Biosensors & Bioelectronics*. **2003**, 18, 1365-1369.

15. Riul, A.; Sousa, C. H.; Malmegrim, R. R.; Santos, R.; Carvalho, A.C.P.L.F.; Fonseca, F.; Olivera, O.; Mattoso, L.H.C. Wine classification by taste sensors made from ultra-thin films and using neural networks. *Sens. Aductors B Chem*. **2004**, 98, 77-82.

16. Beattie, P. D.; Francesso P. O.; Basura, V. I.; Zychocka, K.; Ding, J.; Chuy, C.; Schmeisser, J.; Holdcroft, S. Ion conductivity of proton exchange membranes. *J of Electroanal. Chem.* **2001**, 503, 45-56.

17. Damay, F.; Klein, L. C. Transport properties of Nafion composite membranes for proton-exchange membrane fuel cells. *Solid State Ionics*. **2003**, 162-163, 261-267.

18. Girishkumar, G.; Rettker, M.; Underhile, R.; Binz, D.; Vinodgopal, K.; McGinn, P.; Kamat, P. Single-wall carbon nanotube based proton exchange membrane assembely for hydrogen fuel cells. *Langmuir*. **2005**, 21, 8487-8594.

19. Schlenoff, J.; Li, M.; Ly, H. Stability and Self-Exchange in Alkanethiol Monolayers. *J. Am. Chem. Soc.* **1995**,117, 12528-12536

20. Ulman, A. Formation and Structure of Self-Assembled Monolayers**.** *Chem. Rev.* **1996,** 96, 1533-1554.

21. Flynn, N.; Nga, T.; Tran, T.; Cima, M.;Langer, R. Long-Term Stability of Self-Assembled Monolayers in Biological Media. *Langmuir* **2003**, *19,* 10909-10915.

22. Zhao, Y.; Perez-Segarra, W.; Shi, Q.; Wei, A. Dithiocarbamate Assembly on Gold. *J. Am. Chem. Soc*. **2005**, 127, 7328-7329.

23. Querner, C.; Reiss, P.; Bleuse, J.; Pron, A. Chelating Ligands for Nanocrystals' Surface Functionalization. *J. Am. Chem. Soc.* **2004**, 126, 11574-11582